A LysLysLys-tag as trigger in polynorepinephrine epitope imprinting: the case study of soluble PD-L1 detection in serum by optical-based sensing

Francesca Torrini*, Giada Goletta, Pasquale Palladino, Simona Scarano*, Maria Minunni,

Department of Chemistry 'Ugo Schiff', University of Florence, 50019 Sesto Fiorentino (FI), Italy
*Corresponding authors: francesca.torrini@unifi.it, simona.scarano@unifi.it

Abstract

Polycatecholamines (pCAs)-based molecularly imprinted polymers (MIPs) represent the new performing generation of biocompatible ligand/receptor mimetics. In this context, dealing with MIPs synthesis for bio-macromolecules detection/extraction, one of the critical steps in ensuring effective binding affinity for the parent molecule is the selection of suitable epitopes for pCAs imprinting. To address this challenge, here we investigated the ability of lysine (K) residues to trigger the epitope imprinting process into a polynorepinephrine (PNE) matrix. To this aim, we first designed a set of model epitopes composed of three K and six alanine (A) residues to investigate the influence of each 'KA' combination on the imprinting process and the resulting binding performance by Surface Plasmon Resonance (SPR). Only the case of three flanking K residues in N-terminus arose as an excellent trigger for epitope imprinting. The efficacy of the 3K-tag strategy was then evaluated on two peptide templates belonging to soluble programmed cell death protein 1 ligand (PD-L1), which is of great interest as a cancer biomarker in liquid biopsies. These templates were selected due to their negligible natural ability to be imprinted into the PNE matrix and were modified with 3K-tags, in N-, C-, and N/C- positions, respectively. The SPR sensor developed by exploiting the N-3K tag strategy allowed us to achieve excellent sensitivity (0.31 ± 0.04 ng mL^{-1}) and repeatability ($_{av}CV\% = 4.5$) in human serum samples. This strategy opens new insights both for epitopes' design for pCAs-based mimetics and as triggering tags when native epitopes display negligible imprinting capabilities.

Keywords

Molecularly imprinted polymer, catecholamines, surface plasmon resonance, PD-L1, epitope imprinting, affinity tag

Introduction

Remarkable progress has recently been made in the preparation of imprinted polycatecholamines (pCAs)-based polymers for biomolecular recognition, mainly polydopamine (PDA) and polynorepinephrine (PNE), mimicking antibodies' natural binding (Baldoneschi et al., 2020; Battaglia et al., 2021; Palladino et al., 2018; Torrini et al., 2021; Yin et al., 2015). In particular, the use of short synthetic epitopes (10-15 amino acids) from the primary sequence of parent macromolecule as imprinting templates, allows obtaining selective pCAs-based mimetics for the recognition of a wide variety of biomolecules, irrespective of their size and immunogenicity (Baldoneschi et al., 2020; Khumsap et al., 2021; Lu et al., 2012; Palladino et al., 2018). Dealing with immunogenic targets, one of the first choices in epitope selection is looking at the availability of antigenic sequence/s of the peptide/protein target for which monoclonal antibodies are available. This strategy could aid in selecting well-exposed regions of macromolecules, as suitable epitopes, for molecular imprinting. Nonetheless, from previous studies, we observed that antigen-based epitopes, although well-recognized by specific antibodies, sometimes may be not capable of efficiently imprinting pCAs i.e., do not create template's corresponding cavities in the pCAs matrix (Baldoneschi et al., 2020; Palladino et al., 2018). This behavior may be ascribable to a scarce or absent affinity between the biopolymers (PDA or PNE) and the chemical features of the epitopes' amino acid sequence (a/polarity, acidic/basic prevalence, aromaticity, etc.). Under these circumstances, to the best of our knowledge, the selection of proper epitopes for pCAs imprinting is based on a "try-and-error procedure" that consists in selecting alternative peptides'/proteins' epitopes until effective imprinting is achieved. However, finding alternative epitopes is not always possible, and in general, this approach is not efficient, in terms of time and costs. Thus, there is the need to circumvent this bottleneck in epitope selection for pCAs-based MIPs to definitively widen their real applicability. Among the pCAs' family, here we focused on the use of PNE for MIP synthesis, since our group has recently reported, for the first time, about its impressive superiority versus the most famous PDA when used in bioanalytical abiotic assays, both in biosensing and immune-like assays (Baldoneschi et al., 2020; Battaglia et al., 2021; Torrini et al., 2021; Torrini et al., 2022). In this scenario, for the first time, we designed an innovative and modular imprinting strategy to be applied when epitopes have no imprinting capability or affinity with PNE. Specifically, the study originated from the experimental observation that some epitopes selected for PNE-based MIPs (Baldoneschi et al., 2020; Palladino et al., 2018), although excellently recognized by monoclonal antibodies, are not able to positively interact with the monomer during polymerization to generate the mimetic receptor. This is likely due to an amino acid composition of the epitopes that do not display natural affinity toward the polymer leading to a non-imprinted polymer surface unable to selectively bind the target analyte. We decided to address this issue, using a model system, constituted by a set of peptides/epitopes (9 peptides, Scheme 1) composed of three lysine (K) and six alanine (A) residues, choosing a few representative permutations of K residues among all possible different relative positions and distances along the peptide. These gradual permutations are executed chiefly to study the effect of K itself on the epitopes' imprinting process. The choice of K as a possible trigger was first driven by the existing cooperative effect between catechol and lysine residues, or other amines, that are massively present in mussels' foot proteins and in wet adhesive processes (Fisher et al., 2020; Li et

al., 2017; Li et al., 2020; Maier et al., 2015; Shin et al., 2020). We supposed that the positively charged epsilon-amino group of lysine could modulate the epitopes' affinity for the pCAs, by driving electrostatic interactions with the negatively charged catecholamine structure (upon oxidation to the corresponding ortho-quinones), favoring the incorporation of the K-enriched peptide in the polymeric matrix, somehow recalling a ballast weight added to offset buoyancy. The systematic study of the analytical performances in terms of imprinting and affinity binding of the peptides set 'KA' (Fig. 1a) onto the relative MIPs was accomplished by Surface Plasmon Resonance (SPR) spectroscopy. The first results provide important information about the role of key amino acids, here K, as triggering tags for epitopes with a negligible affinity for PNE during MIP synthesis. Additionally, to demonstrate the transferability of the result observed to a real diagnostic case, programmed cell death protein 1 ligand (PD-L1) was investigated. PD-L1 is a glycoprotein constituted by 290-amino acid (Lawson et al., 2019), which is commonly overexpressed on tumor cells. It binds the PD-1 receptor, a transmembrane protein located mainly on T and B cell surfaces, with the primary function to evade the host immune system surveillance promoting tumorigenesis (Fessas et al., 2017; Jiang et al., 2019; Tsoukalas et al., 2019; Zhang et al., 2020). Besides, recent studies have also revealed that PD-L1 is present as a soluble form in blood samples, secreted or cleaved from positive cells, even if the exact role/provenience and the correlation to the membrane-bound PD-L1 are yet poorly disclosed (Zhu et al., 2017). Indeed, the circulating soluble PD-L1 (sPD-L1) fraction is currently under consideration for clinical trials as a potential predictive and prognostic cancer biomarker in liquid biopsies for several solid cancers e.g., lung cancer (Cheng et al., 2022; Honrubia-Peris et al., 2021), renal cell cancer (Mahoney et al., 2022), melanoma (Mahoney et al., 2022; Zhou et al., 2017), hepatocellular carcinoma (Finkelmeier et al., 2016), gastric cancer (Imai et al., 2020), pancreatic cancer (Kruger et al., 2017), and primary central nervous system lymphoma (PCNSL) (Cho et al., 2020; Oh et al., 2021). In this context, we selected two peptide sequences, designed respectively on the extracellular domain and on the full-length of PD-L1, that have shown negligible ability/affinity to PNE imprinting. The triggering effect associated with the presence of the 3K-tag was eventually explored on PD-L1 sequences, here representing a case study for further confirmation of the evidence achieved in the model study. Finally, the most promising mimetic receptor was embedded in the sensing platform (SPR) to directly quantify PD-L1 both in buffer and in spiked human serum, covering the median human level of this emerging biomarker in putative real samples, according to Cho et al. (2020) (median pathologic level 0.429 ng mL^{-1}, range: 0.324-0.757 ng mL^{-1}; median healthy level 0.364 ng mL^{-1}, range: 0.329-0.390 ng mL^{-1}).

2. Material and Methods

2.1 Chemicals and reagents

L-norepinephrine hydrochloride (NE, ≧ 98.0%), tris(hydroxymethyl)aminomethane hydrochloride (Tris-HCl, ≧ 99.0%), 4-(2-Hydroxyethyl)piperazine-1-ethanesulfonic acid (HEPES), disodium hydrogen phosphate dihydrate, potassium chloride, sodium chloride, sodium dihydrogen phosphate, hydrochloric acid, acetic acid

(≧ 99.7%), sodium dodecyl sulfate (SDS), polyoxyethylene sorbitan monooleate (Tween-20), lysine, L-cysteine hydrochloride monohydrate, human serum albumin (HSA) and sterile-filtered human serum (from human male AB plasma) were all purchased from Merck (Darmstadt, Germany). 10K Amicon® Ultra centrifugal filter units were obtained from Millipore Corp. (Bedford, MA, USA). All the peptide sequences with a HPLC purity above 95.0% here listed: PEP1-7 reported in Fig. 1a; pd-l1$_{ex}$ (MW = 1181.39 g mol^{-1}), C-3K pd-l1$_{ex}$ (MW = 1566.89 g mol^{-1}), N-3K pd-l1$_{ex}$ (MW = 1565.91 g mol^{-1}), NC-3K pd-l1$_{ex}$, (MW = 1951.41 g mol^{-1}), pd-l1$_{in}$ (MW = 1315.39 g mol^{-1}), C-3K pd-l1$_{in}$ (MW = 1699.91 g mol^{-1}), N-3K pd-l1$_{in}$ (MW = 1699.91 g mol^{-1}), NC-3K pd-l1$_{in}$ (MW = 2084.43 g mol^{-1}) sequences reported in Fig. 4a, and human PD-L1 (Phe19-Thr239 residues plus a C-terminal His-tag, MW ~ 31-35 kDa. UniProtKB Accession # Q9NZQ7-1) were provided by GenScript (Leiden, Netherlands). Ultrapure Milli-Q™ water (R ≧ 18.2 MΩ • cm) was used to prepare all the buffer solutions. Phosphate buffered saline (PBS composition: 140 mM NaCl, 2.68 mM KCl, 3.56 mM NaH_2PO_4, 6.44 mM Na_2HPO_4, pH 7.4) and PBS pH = 7.8 plus 0.05% SDS were used as dilution and running buffer respectively during the peptides ('AK' set, all pd-l1$_{ex}$ and pd-l1$_{in}$ sequences) and PD-L1 SPR analyses. Buffered solutions were filtered through a microporous filter (0.22 μm). All chemicals used were of analytical grade. Gold sensor chips were obtained from Cytivia Sweden AB (Uppsala). SPR measurements were all carried out by using Biacore X-100 instrumentation (Cytivia Sweden AB, Uppsala).

2.2 Preparation of PNE-based MIPs

PNE-based MIPs (template = 400 μmol L^{-1}) were directly synthesized on the sensor chips following a previously published well-assessed procedure (Torrini et al., 2021). All the polymeric surfaces were passivated with a solution constituted by 1 mM lysine, 1 mM L-cysteine hydrochloride monohydrate, and 1 mM tris(hydroxymethyl)aminomethane hydrochloride at 25 °C (for measurements in buffer solution), or with a 1 mM 11-mercaptoundecanoic acid (MUA), and 6-mercapto-1-hexanol (MCH) in a water/ethanol solution (80:20, v/v) (for measurements in human serum). A washing step with acetic acid (5 % v/v) and deionized water was used to remove the template from the binding cavities of MIPs. Non-imprinted polymers (NIPs) were prepared following the same experimental procedure for MIPs, without template addition.

2.3 SPR interaction analysis of the 'KA' peptides with MIPs$_{KA}$

PEP 1-7 (Fig. 1a) binding capacities *versus* the relative MIP$_{1-7}$ surfaces were evaluated by performing single-cycle kinetic (SCK) analyses (flow rate: 5.00 μL min^{-1}, T = 25.0 ± 0.5 °C), consisting of five sequential injections of increasing target concentrations over the receptor surface, bypassing the regeneration step among different measurement cycles. The peptides were diluted in PBS pH 7.4 in a concentration range spanning from 3.5 μmol L^{-1} to 60 μmol L^{-1} and were injected over the MIP surface for 120 s each, followed by a 30 s dissociation phase with the running buffer. After each measuring cycle, the MIP binding cavities were regenerated by injecting short (24 s) pulses of 20 mM HCl. Data processing was carried out with Origin 2021b using a one-site binding fitting model. The equation applied to generate the affinity calibration curves was RU

= (R_{max} x [Peptide])/(K_D + [Peptide]), where R_{max} is the maximum response (RU), and the K_D is the Peptide-MIP equilibrium dissociation constant. Considering the larger response reported in Fig. 1 for PEP 1-4 than for PEP 5-7, the imprinting factor (IF), calculated as MIP/NIP signal ratio (Fig. 2), was estimated only for MIP_{1-4} surfaces by injecting the corresponding template peptide at a fixed concentration (15.00 µmol L^{-1}, injections of 120 s in manual run mode) on both the relative MIP and a reference NIP surface. The $MIPs_{1-4}$ selectivity towards the specific target analyte was evaluated by cross-testing all the other 'KA' peptides on $MIPs_{1-4}$ surfaces (Fig. 3).

2.4 Epitope selection and PD-L1 detection in buffer

Two peptide sequences belonging to PD-L1 were selected respectively in the extracellular domain and in the cytoplasmatic domain (31-residue) from the full-length human PD-L1 (UniprotKB – Q9NZQ7) as templates for PNE epitope imprinting, hereafter referred to as pd-l1$_{ex}$ and pd-l1$_{in}$, respectively (Fig. 4a). Specifically, pd-l1$_{ex}$ (^{19}FTVTVPKDLY^{28}-NH_2) was selected in the N-terminal domain. pd-l1$_{in}$ (^{280}KKQSDTHLEET^{290}) was selected in the C-terminus domain by exploiting epitope mapping information on existing mAbs for laboratory use, as reported by Lawson et al. (2020), and matches (partly or fully) natural epitopes specifically recognized by rabbit mAbs (VENTANA PD-L1 - SP263 and SP142 clones' epitope: ^{284}DTHLEET^{290}; PD-L1 XP® E1L3N® clone's epitope: ^{280}KKQSDTHLEET^{290}) (Lawson et al., 2020; Smith, 2016). Moreover, additional peptides modified with the three lysine (K) -tag were designed and acquired: C-3K pd-l1$_{ex}$/pd-l1$_{in}$, N-3K pd-l1$_{ex}$/pd-l1$_{in}$, NC-6K pd-l1$_{ex}$/pd-l1$_{in}$. All the peptides were calibrated in the binding buffer on the relative MIP within 0.094-15 µmol L^{-1} by setting the same analysis method of 'KA' peptides (Paragraph 2.3). PD-L1 whole protein was tested in buffer within 0.25 and 10 µg L^{-1} on the selected $MIP_{pd\text{-}l1ex}$ (contact time of 120 s for each injection); after each sample measurement, the MIP surface was regenerated with a single-shot injection (contact time: 24 s) of 10 mM glycine pH 1.5. The selectivity of the MIP was tested against HSA (320 mol L^{-1}, injection of 120 s, flow rate: 5.00 µL min^{-1}), the most abundant protein in human serum (Fanali et al., 2012).

2.5 PD-L1 detection in human serum by SPR

Human serum samples were reinforced with PD-L1 and then cleaned up using 10K Amicon centrifugal devices (14,000 □ g for 15 min). For signal amplification in the lower ng mL^{-1} concentration range, the SPR protocol was optimized as follows: contact time of 1200 s; PD-L1 accumulation was performed by three sequential injections of 400 s each. The analytical parameters, namely limit of detection (LOD) and limit of quantitation (LOQ), were established both in buffer and human serum using the following equation LOD = 3σ □ K_D/R_{max} and LOQ = 10σ □ K_D/R_{max}, where sigma (σ) is the standard deviation of the mean signal of the blank solution.

3. Results and discussion

3.1 3K- tag effect on PNE-MIP performances

In the first part of the study, we addressed the systematic study of the K residues' influence on a model set of peptides 'KA' in triggering the PNE imprinting process *via* SPR. We investigated the specific K effect on such peptide imprinting and interaction by changing the position and the spacing among K residues (Fig. 1a), which appear virtually moved towards the N- or C-terminus to finally create an ending 3K-tag (PEP 4 and 7, respectively). Each peptide was firstly used to imprint the relative PNE-based MIP, then the affinity binding characteristics, for each MIP-template combination, were evaluated by single-cycle kinetic (SCK) method available on Biacore X-100 control software. As reported in Figs. 1b-c, starting from the calibration of PEP-1 (KA_3KA_3K, black line), with a balanced distribution of the three K, the behavior of all the other peptides is grouped in two well-distinguished trends in terms of imprinting/binding capacity: the blue one (PEPs 2-3-4) and the red one (PEPs 5-6-7). This suggests a clear positive correlation with a K triggering effect on MIPs' binding performances, moving from PEP-1, in which K are equidistributed, up to PEPs 2-4, which have K grouped at the N-terminus. Indeed, we observed that the K residues are able to strongly and positively influence the imprinting process (as also demonstrated by the equilibrium dissociation constant K_D reported in Table S1), confirming the absolute propensity of the PNE polymer in incorporating K residues. Conversely, when the K residues are grouped at the C-terminus (PEPs 5-7), a negative effect on the MIPs' binding performances is observed. Such results, unexpectedly, indicate that the 3K-tag is able to trigger the imprinting process only if located at the N-terminal region of the peptide. For this reason, taking into account the above considerations, we focused on PEPs 1-4 for further investigation.

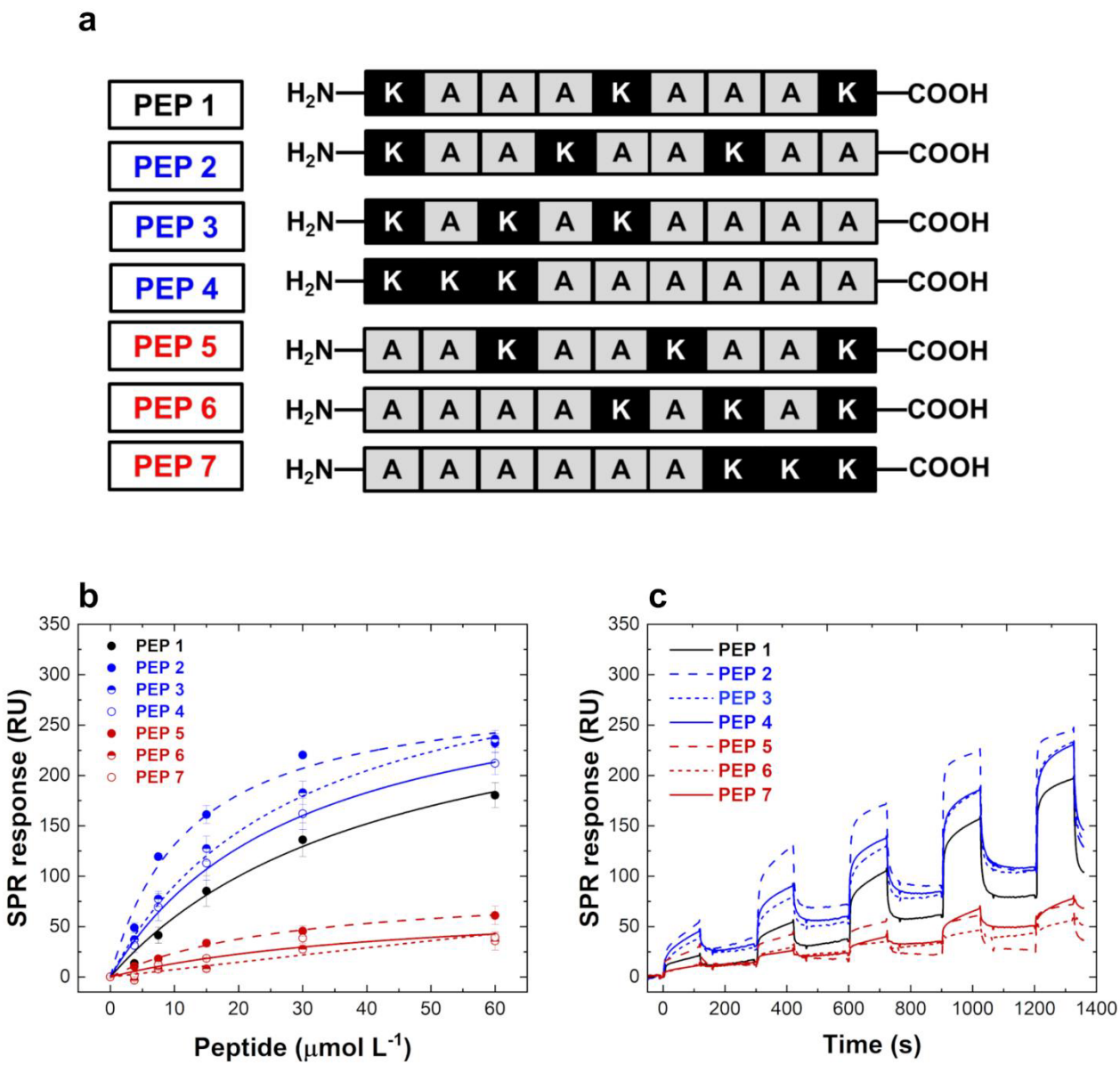

Fig. 1 (a) Peptide sequences set 'KA'. PEP-1 (KA_3KA_3K), PEP-2 ($KA_2KA_2KA_2$), PEP-3 ($KAKAKA_4$), PEP-4 (K_3A_6), PEP-5 ($A_2KA_2KA_2K$), PEP-6 (A_4KAKAK), PEP-7 (A_6K_3). (b) Affinity calibration curves and (c) binding sensorgrams by single-cycle kinetic (SCK) analysis performed on $MIPs_{1-7}$ by testing the PEPs 1-7 within the concentration range 3.5-60 µmol L^{-1}. The calibration curves were obtained by plotting the binding level against the peptide concentrations tested and were fitted with a one-site binding model to extrapolate the K_D values and R_{max} (Table S1).

3.2 Selectivity of the MIPs

The success of the imprinting process was assessed in terms of imprinting factor and selectivity. Mimetic receptors imprinted with PEPs 1-4, respectively, were evaluated by comparing binding SPR signals of PEPs 1-4 against those obtained on control non-imprinted polymers (NIPs). The efficiency of $MIPs_{1-4}$ over the NIP was expressed as imprinting factors ($IF = MIP_{SPR\ signals}/NIP_{SPRsignals}$). The results displayed in Fig. 2 highlight

the effectiveness of the imprinting process, all the MIPs show a significant binding toward the relative target, MIP_3 and MIP_4 exhibited also very good repeatability.

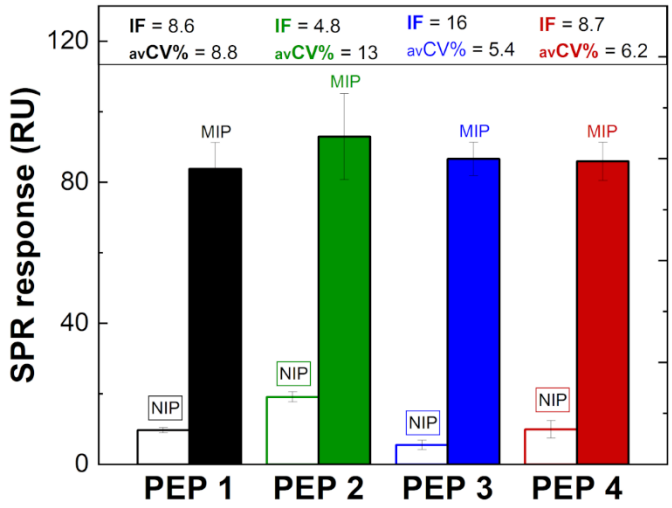

Fig. 2 Comparison of PEPs 1-4 SPR responses on MIPs and NIP surfaces. All the peptides were tested, on both surfaces, at a fixed concentration of 15 µmol L^{-1}. The bar chart indicates $RU_{mean} \pm$ SD recorded in triplicate for each peptide on the corresponding mimetic receptor.

Moreover, the cross-reactivity of PEPs 1-4 for all the other non-corresponding MIPs was also assessed (Fig. 3). All the peptides/templates (PEPs 1-4) tested are differentiated only for the arrangement of the amino acids 'AK' (Fig. 1a), thus preserving their number (3 and 6, respectively), molecular weight, net charge, and isoelectric point. The selectivity of each MIP for its target is significant for MIP_4, somehow indicating that the imprinting of PEP-4, bearing three K residues at N-terminus (N-3K), confers to the recognition cavities the shape and the ability to discriminate PEP-4 sequence among all the other peptide sequences tested, in which the 3K residues are "scrambled" along the sequence. This very encouraging evidence supports further investigation of this effect on a biologically relevant model system. Thus, this epitope imprinting strategy was applied to the glycoprotein PD-L1.

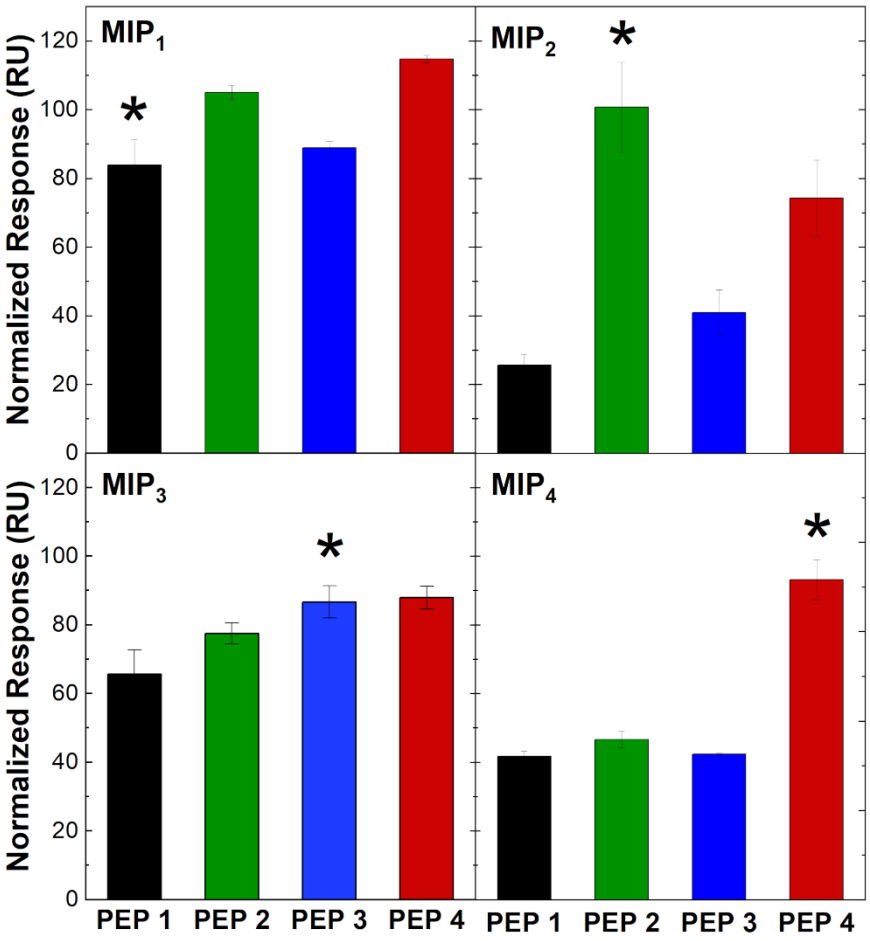

Fig. 3 Cross-reactivity binding of PEPs 1-4 tested on MIPs$_{1\text{-}4}$. The template/target peptide for each MIP is marked with an asterisk.

3.3 3K-tag driven epitope imprinting strategy for PD-L1 detection

The applicability of the 3K-tag, which has displayed a positively triggering effect on MIP synthesis when located in the N-terminal domain of the 'KA' model peptide, was expanded to study a real case.

Thus, we moved from our model system to a real biomarker of interest in clinical diagnostic, PD-L1. Two peptide sequences belonging to the full-length human PD-L1 were preliminarily selected for PD-L1 detection. This is the case of the C-terminus undecapeptide (^{280}KKQSDTHLEET^{290}, pd-l1$_{in}$) that, albeit selected on a recognition site for mAbs, displays negligible PNE-imprinting/binding ability as shown by SPR measurements (Fig. 4 and Table S2). The same problem was faced when the epitope was selected in the N-terminal domain (^{19}FTVTVPKDLY^{28}-NH$_2$, pd-l1$_{ex}$), a well-exposed portion of the full-length human PD-L1 (Figs. 4b-c and Table S2). Therefore, the epitopes pd-l1$_{ex}$/pd-l1$_{in}$ underwent modifications with the 3K-tag at the N- and/or C-terminus (sequences in Fig. 4a) and were used to synthesize PNE-based MIPs.

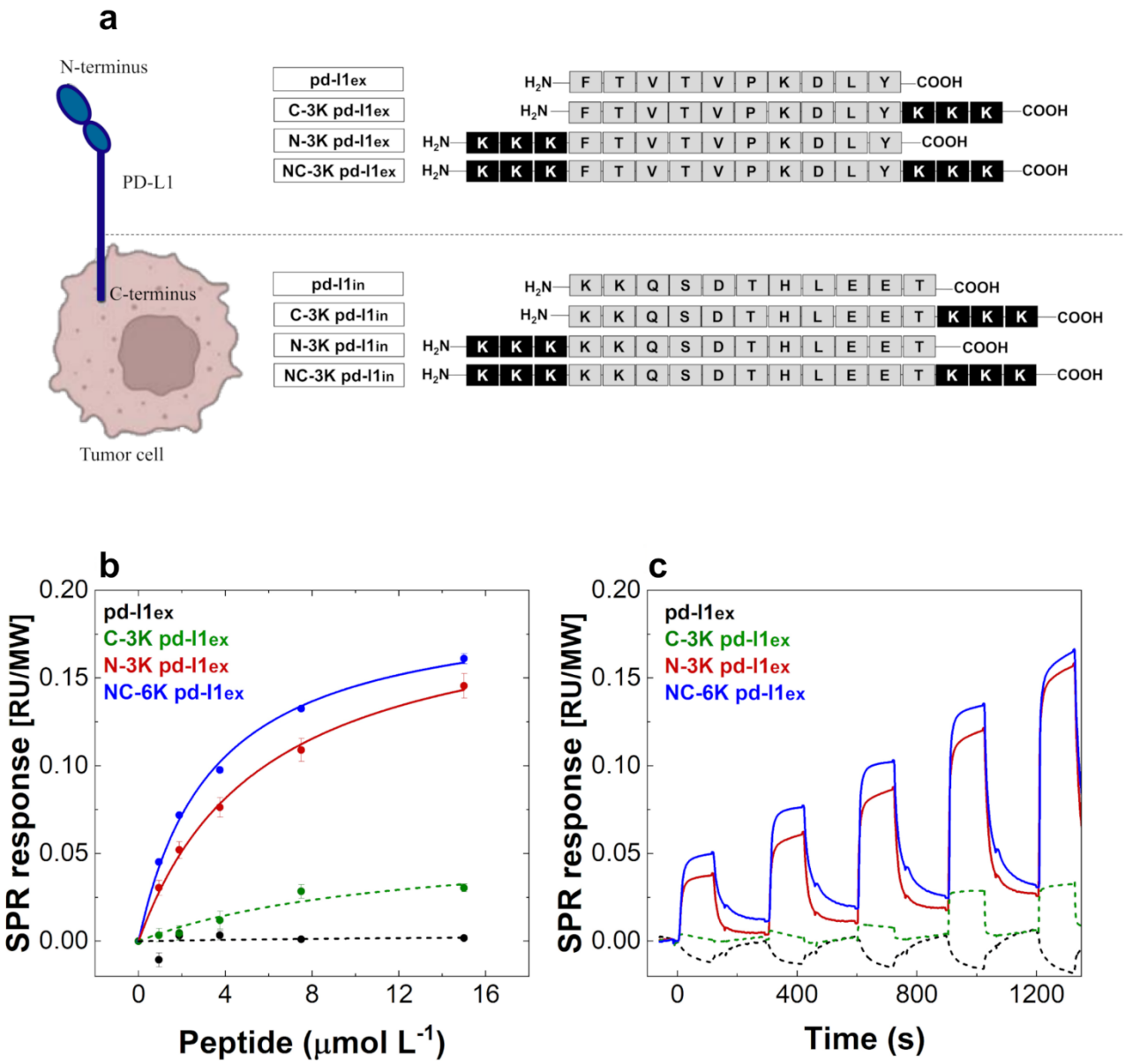

Fig. 4 (a) Epitopes' sequences: pd-l1$_{ex}$/ pd-l1$_{in}$, C-3K pd-l1$_{ex}$/ pd-l1$_{in}$, N-3K pd-l1$_{ex}$/ pd-l1$_{in}$, NC-3K pd-l1$_{ex}$/ pd-l1$_{in}$. (b) Dose-response curves and (c) representative sensorgrams for all the peptides over their respective MIPs. SPR responses (RU), obtained by single-cycle kinetic (SCK) method with increasing peptide concentrations ranging from 0.94 to 15 µmol L^{-1}, were expressed as normalized values (RU/MW) (see material and method) after blank subtraction. Each point is representative of three replicates ($RU_{mean} \pm SD$).

The binding affinities were tested by SPR (Figs. 4b and S1a) and all the signals (RU) recorded were normalized with respect to the molecular weight (MW) of the unmodified targets [RU/MW] to take into account the MW increase in weight induced by the 3K/6K tags. Once again, a high binding was observed when the 3K-tag is added at the N-terminus, or in combination with a second 3K at the C-terminus (NC-6K), which seems to promote a synergistic effect corresponding to a further affinity increase (K_D value, Table S2). No appreciable

binding occurs when the 3K, alone, is added at the C-terminus (C-3K), confirming the evidence that arose from the model peptide PEP-7. Although the apparent cooperative effect of the NC-6K-tag is of great interest and deserves further studies, here we focused on the key role of the single N-3K-tag.

Actually, our primary goal is first to trigger the epitopes' imprinting during PNE polymerization, then to obtain the successful recognition of the non-modified real target, which does not naturally contain the 3K-tag. Thus, once obtained several PNE-based MIPs (Fig. 4a), these were tested in their ability to bind first the unmodified peptides (without the 3K-tags) and then the native PD-L1 whole molecule. Accordingly, to prove the real benefit of the N-3K-tag in the pd-l1$_{ex}$/pd-l1$_{in}$ epitope imprinting process, we tested the ability of the native unmodified peptides (pd-l1$_{ex}$/pd-l1$_{in}$,) to bind the different MIPs (MIP$_{pd\text{-}l1_{ex}/pd\text{-}l1_{in}}$, C-3K MIP$_{pd\text{-}l1_{ex}/pd\text{-}l1_{in}}$, and N-3K MIP$_{pd\text{-}l1_{ex}/pd\text{-}l1_{in}}$), imprinted with the corresponding peptides/templates modified with K-tags (Fig. 4a). This is a key prerequisite for a real application of this strategy to native proteins, which do not carry targeted modifications. Successfully, the SPR responses for the native target analytes impressively increase by moving from MIP$_{pd\text{-}l1_{ex}/pd\text{-}l1_{in}}$ (no binding, black bar) to N-3K MIP$_{pd\text{-}l1_{ex}/pd\text{-}l1_{in}}$ (highest binding, red bar) (Fig. 5a; Fig. S2 shows that similar results are obtained also for MIP$_{pd\text{-}l1_{in}}$). The presence of the 3K-tag at the N-terminal allows the imprinting and the rebinding of the epitopes, which instead were unable to imprint/rebind the polymer without such triplet, corroborating the evidence obtained with the set of 'AK' peptides. To go ahead with the detection of PD-L1 whole protein, the mimetic receptor was imprinted using only pd-l1$_{ex}$ as epitope, since the commercially available protein includes only the extracellular domain (Phe19-Thr239 residues). A positive trend was observed, moving from MIP$_{pd\text{-}l1_{ex}}$ to N-3K MIP$_{pd\text{-}l1_{ex}}$ by testing both the pd-l1$_{ex}$ peptide (Fig. 5a) and the PD-L1 whole protein (Fig. 5b) is reported. These findings demonstrate that the insertion of the N-3K-tag along the pd-l1$_{ex}$ sequence plays a crucial role, not only by increasing the affinity of the selected imprinting epitope but also, more importantly, by eliciting an effective recognition of the PD-L1 protein. The large difference between the signal values observed for the pd-l1$_{ex}$ (Fig. 5a) and PD-L1 (Fig. 5b) binding to the relative MIPs is mainly determined by the large difference between their molecular weights (pd-l1$_{ex}$: 1181.39 Da; PD-L1: ~ 31 kDa), since SPR is an optical technique sensitive to refractive index (RI) changes and here the higher MW of the analytes induces bigger RI changes at the MIP surface. For each native target analyte (pd-l1$_{ex}$ and PD-L1), the relative signal variation (ΔRU) achieved using modified epitopes template (N-3K and C-3K) with respect to unmodified ones (expressed as ratio $\left|\frac{RU_{modified\ template}}{RU_{native\ target}}\right|$, was estimated ($\Delta RU_{C\text{-}3K(pd\text{-}l1ex)} = 0.6$, $\Delta RU_{C\text{-}3K(pd\text{-}l1ex)} = 2$; $\Delta RU_{C\text{-}3K(PD\text{-}L1)} = 0.09$, $\Delta RU_{N\text{-}3K(PD\text{-}L1)} = 143$).

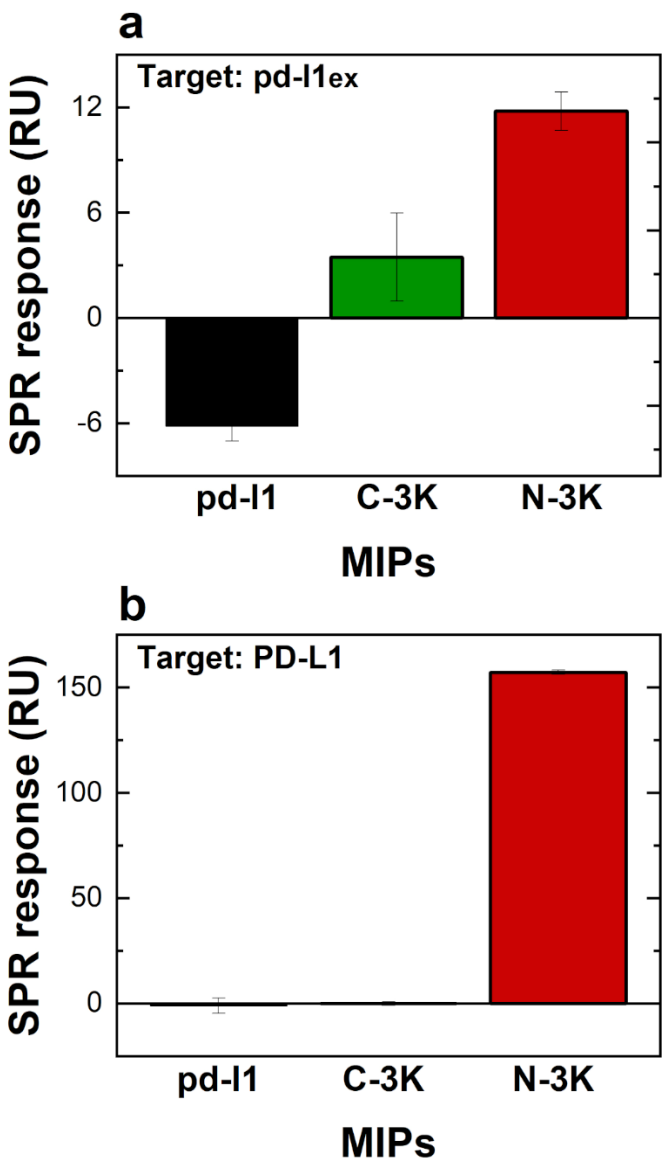

Fig. 5 SPR responses (RU_{mean} ± SD) recorded for the binding interactions between (a) pd-l1ex peptide (15 µmol L^{-1}) or (b) the whole macromolecule PD-L1 (3 µg mL^{-1}, 97 nmol L^{-1}) and the MIPs imprinted with three different epitopes (Fig. 4a: pd-l1ex, C-3K pd-l1ex, and N-3K pd-l1ex).

3.4 Direct PD-L1 detection in buffer and human serum

Finally, the PNE-based MIP imprinted with the N-3K pd-l1ex template (Fig. 6a) was used to develop a direct and quantitative SPR assay for the detection of the soluble fraction of PD-L1, glycoprotein of interest in clinical diagnostic, firstly in buffer and then in human serum samples (Figs. S3 and 6b). The measurements in buffer were performed by injecting different PD-L1 concentrations (contact time 120 s at 5 µL min^{-1}), giving well-measurable signals within the investigated concentration interval (0.25-10 µg mL^{-1}). The sensor displayed excellent repeatability ($_{av}$CV% = 2.6%), achieving a limit of detection (LOD) and quantification (LOQ) of 4.2 ± 0.4 ng mL^{-1} and 14.0 ± 1.2 ng mL^{-1}, respectively. The MIP-based sensor displayed a dynamic range up to 10

µg mL^{-1} PD-L1, with a linear range from 0.25 to 1.0 µg mL^{-1}. Data in Fig.S3 were fitted with a one-site binding model (Paragraph 2.3), estimating the parameters K_D = 2.5 ± 0.22 µg mL^{-1} and R_{max}= 273 ± 10 µg mL^{-1} (R^2 = 0.992).

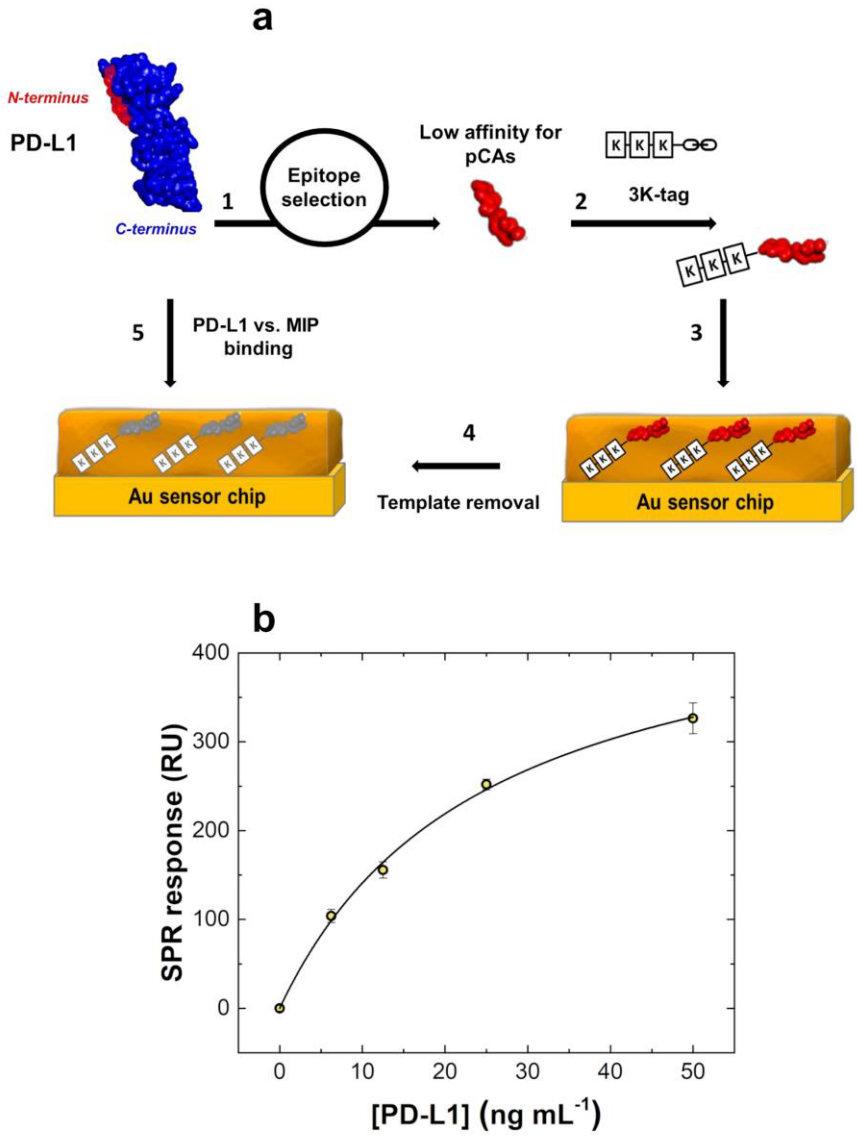

Fig. 6 (a) Scheme of the epitope imprinting process for PD-L1 detection. (b) Direct MIP-based assay for PD-L1 detection in spiked human serum samples (6.0-50 ng mL^{-1}). Each point is representative of three measurements (RUmean ± SD). The SPR signal of the blank was subtracted from each measurement.

The selectivity of the PD-L1 sensor was first assessed by comparing the response against the major potential interfering analyte (blood concentration level 50 g L^{-1}), i.e., human serum albumin (HSA). As reported in Fig. S4, a negligible non-specific response was recorded, compared to PD-L1 binding onto the N-3K $MIP_{pd\text{-}l1ex}$ at

the same concentration (320 nmol L^{-1}). These results confirm the excellent selectivity of the N-3K $MIP_{pd\text{-}l1ex}$ previously observed with the 'KA' peptides (Fig. 3). The SPR direct assay was also performed in human serum spiked with known soluble PD-L1 concentrations (6.0-50 ng mL^{-1}) for its detection in real-time. At this stage, we decided to introduce a simple and fast clean-up process to guarantee the absence of any non-specific signal (see material and methods). Then, serum samples were injected over the sensor by using an optimized binding protocol involving a prolonged incubation (400 s at a flow rate of 5 µL min^{-1}) and a sample accumulation step on the surface to improve the sensitivity of the assay in the real matrix (see material and methods). Fig. 6b displays the SPR signals recorded against PD-L1 concentrations (ng mL^{-1}). The calculated LOD and LOQ resulted equal to 0.31 ± 0.04 ng mL^{-1} and 1.08 ± 0.14 ng mL^{-1}, respectively, and were determined by 3σ and 10σ interpolation in the curve (one-site binding model fitting, R^2 = 0.997), together with good repeatability ($_{av}$CV% = 4.5%). The sensitivity achieved by the direct detection of PD-L1 in human serum via a MIP-based sensing platform is in line with the clinical reference values reported by Cho et al. (2020).

Conclusions

In this study, we have developed an extremely effective strategy to modify epitopes in order to synthesize molecularly imprinted polymers (MIPs) for the detection of biologically relevant analytes and to overcome the difficulties encountered with imprinting aa-based templates (epitopes) that appear reluctant to pCAs-based imprinting, here polynorepinephrine (PNE), failing to generate a selective binding polymer. The investigation of 'KA' model peptides, consisting of 6A and 3K, rationally designed in terms of distance and relative position along the sequence among all the possible permutations, allowed us to identify and select an extremely active 3K sequence in triggering the template imprinting and subsequent epitope recognition also without any modification, as naturally occurring. The unpredicted result is the evidence that only the N-terminal addition of the 3K-tag shows the ability to elicit the imprinting. This finding is, alone, of great interest and deserves further investigation to confirm a natural propensity of PNE in imprinting the amino acid templates following the N to C direction. If extended to any peptide sequence, this key feature surely will open new exciting scenarios in the field of CAs-based MIPs (e.g., by comparing this behavior on PDA) for biomolecules detection/extraction. Not least, the investigation of other amino acid tags and their effects on CAs-based and other soft biopolymers is a horizon that inspires us and is now extremely necessary to go deeper in describing these intriguing materials for bio-detection. In a real diagnostic case, the "induced imprinting" strategy applied to PD-L1 templates, failing native epitopes for PNE imprinting, which allowed us to successfully generate MIPs for the direct detection of this emerging cancer biomarker. Successfully, the addition of the N-3K tag to these epitopes drastically evoked the ability to 'force' the imprinting of the recognition sequence on the polymer matrix, obtaining well-functioning imprinted surfaces able to rebind also the unmodified templates (without the tag), and the whole target protein both in buffer and serum. The analytical performances resulted in line with the clinical reference values, otherwise impossible by using pCAs-based MIPs produced with no modified epitopes. The apparent general utility of this simple and new method expands the applicability of MIPs, offering a better synthetic alternative to biological antibodies and receptors in bioassays.

Acknowledgments

Authors thank the Italian Ministry of Health for funding within the call "Research and training/information 2020 program on drugs, medical substances, and practices that can be used for doping purposes and for health protection in sporting activities". The authors also thank the Ministry of Education, University and Research (MIUR), for the project "Dipartimenti di Eccellenza 2018–2022".

References

Baldoneschi,V., Palladino, P., Banchini, M., Minunni, M., Scarano, S., 2020. Norepinephrine as new functional monomer for molecular imprinting: An applicative study for the optical sensing of cardiac biomarkers. Biosens Bioelectron. 157, 112161.

Battaglia, F., Baldoneschi, V., Meucci, V., Intorre, L., Minunni, M., Scarano, S., 2021. Detection of canine and equine procalcitonin for sepsis diagnosis in veterinary clinic by the development of novel MIP-based SPR biosensors. Talanta 230,122347.

Cheng, Y., Wang, C., Wang, Y., Dai, L., 2022. Soluble PD-L1 as a predictive biomarker in lung cancer: a systematic review and meta-analysis. Future Oncol. 18, 261-273.

Cho. I., Lee, H., Yoon, S.E., Ryu, K.J., Ko, Y.H., Kim, W.S., Kim, S.J., 2020. Serum levels of soluble programmed death-ligand 1 (sPD-L1) in patients with primary central nervous system diffuse large B-cell lymphoma. BMC Cancer 13, 120.

Fanali, G., di Masi, A., Trezza, V., Marino, M., Fasano, M., Ascenzi, P., 2012. Human serum albumin: from bench to bedside. Mol Aspects Med. 33, 209-90.

Fessas, P., Lee, H., Ikemizu, S., Janowitz, T., 2017. A molecular and preclinical comparison of the PD-1-targeted T-cell checkpoint inhibitors nivolumab and pembrolizumab. Semin Oncol. 44, 136-140.

Finkelmeier, F., Canli, Ö., Tal, A., Pleli, T., Trojan, J., Schmidt, M., Kronenberger, B., Zeuzem, S., Piiper, A., Greten, F.R, Waidmann, O., 2016. High levels of the soluble programmed death-ligand (sPD-L1) identify hepatocellular carcinoma patients with a poor prognosis. Eur J Cancer. 59, 152-159.

Fischer, L., Strzelczyk. AK., Wedler, N., Kropf, C., Schmidt, S., Hartmann, L., 2020. Sequence-defined positioning of amine and amide residues to control catechol driven wet adhesion. Chem Sci. 11, 9919-9924.

Honrubia-Peris, B., Garde-Noguera, J., García-Sánchez, J., Piera-Molons, N., Llombart-Cussac, A., Fernández-Murga, M.L., 2021. Soluble Biomarkers with Prognostic and Predictive Value in Advanced Non-Small Cell Lung Cancer Treated with Immunotherapy. Cancers (Basel) 13, 4280.

Imai, Y., Chiba, T., Kondo, T., Kanzaki, H., Kanayama, K., Ao, J., Kojima, R., Kusakabe, Y., Nakamura, M., Saito, T., Nakagawa, R., Suzuki, E., Nakamoto, S., Muroyama, R., Tawada, A., Matsumura, T., Nakagawa,

T., Kato, J., Kotani, A., Matsubara, H., Kato, N., 2020. Interferon-γ induced PD-L1 expression and soluble PD-L1 production in gastric cancer. Oncol Lett. 2020 Sep;20(3):2161-2168.

Jiang, Y., Chen, M., Nie. H., Yuan. Y. 2019. PD-1 and PD-L1 in cancer immunotherapy: clinical implications and future considerations. Hum Vaccin Immunother. 15, 1111-1122.

Khumsap, T., Bamrungsap, S., Thu, V.T., Nguyen, L.T., 2021. Epitope-imprinted polydopamine electrochemical sensor for ovalbumin detection. Bioelectrochemistry 140, 107805.

Kruger, S., Legenstein, M.L, Rösgen, V., Haas, M., Modest, D.P., Westphalen, C.B., Ormanns, S., Kirchner, T., Heinemann, V., Holdenrieder, S., Boeck, S., 2017. Serum levels of soluble programmed death protein 1 (sPD-1) and soluble programmed death ligand 1 (sPD-L1) in advanced pancreatic cancer. Oncoimmunology 6, e1310358.

Lawson, N.L, Dix, C.I, Scorer, P.W, Stubbs, C.J, Wong, E., Hutchinson, L., McCall, E.J, Schimpl, M., DeVries, E., Walker, J., Williams, G.H, Hunt, J., Barker, C., 2020. Mapping the binding sites of antibodies utilized in programmed cell death ligand-1 predictive immunohistochemical assays for use with immuno-oncology therapies. Mod. Pathol. 33, 518-530.

Li, Y., Liang, C., Gao, L., Li, S., Zhang, Y., Zhang, J., Cao, Y., 2017. Hidden complexity of synergistic roles of Dopa and lysine for strong wet adhesion. Mater. Chem. Front. 1, 2664-2668.

Li, Y., Cheng, J., Delparastan, P., Wang, H., Sigg, S.J., DeFrates, K.G., Cao, Y., Messersmith, P.B., 2020. Molecular design principles of Lysine-DOPA wet adhesion. Nat Commun 11, 3895.

Lu, CH., Zhang, Y., Tang, SF., Fang, ZB., Yang, HH., Chen, X., Chen, GN., 2012. Sensing HIV related protein using epitope imprinted hydrophilic polymer coated quartz crystal microbalance. Biosens Bioelectron. 31, 439-44.

Mahoney, K.M, Ross-Macdonald, P., Yuan, L., Song, L., Veras, E., Wind-Rotolo, M., McDermott, D.F, Hodi, S.F, Choueiri T.K, Freeman G.J., 2022. Soluble PD-L1 as an early marker of progressive disease on nivolumab. J Immunother Cancer 10, e003527

Maier, G.P, Rapp, M.V, Waite, JH., Israelachvili, J.N, Butler, A. 2015. BIOLOGICAL ADHESIVES. Adaptive synergy between catechol and lysine promotes wet adhesion by surface salt displacement. Science 349, 628-32.

Oh, S.Y., Kim, S., Keam, B., Kim, T.M., Kim, D.W., Heo, D.S., 2021. Soluble PD-L1 is a predictive and prognostic biomarker in advanced cancer patients who receive immune checkpoint blockade treatment. Sci Rep. 11, 19712.

Palladino, P., Portella, L., Colonna, G., Raucci, R., Saviano, G., Rossi, F., Napolitano, M., Scala, S., Castello, G., Costantini, S., 2012. The N-terminal Region of CXCL11 as Structural Template for CXCR3 Molecular Recognition: Synthesis, Conformational Analysis, and Binding Studies. Chem. Biol. Drug Des., 80, 254-265.

Palladino, P., Minunni, M., Scarano, S., 2018. Cardiac Troponin T capture and detection in real-time via epitope-imprinted polymer and optical biosensing. Biosens Bioelectron. 106, 93-98.

Shin, M., Shin, J.Y., Kim, K., Yang, B., Han, J.W., Kim, N.K., Cha, H.J., 2020. The position of lysine controls the catechol-mediated surface adhesion and cohesion in underwater mussel adhesion. J Colloid Interface Sci. 563, 168-176.

Smith, J., Robida, M.D, Acosta, K., Vennapusa, B., Mistry, A., Martin, G., Yates, A., Hnatyszyn, HJ., 2016. Quantitative and qualitative characterization of Two PD-L1 clones: SP263 and E1L3N. Diagn Pathol. 11, 44.

Torrini, F., Palladino, P., Baldoneschi, V., Scarano, S., Minunni, M., 2021. Sensitive 'two-steps' competitive assay for gonadotropin-releasing hormone detection via SPR biosensing and polynorepinephrine-based molecularly imprinted polymer. Anal Chim Acta. 1161, 338481.

Torrini, F., Caponi, L., Bertolini, A., Palladino, P., Cipolli, F., Saba, A., Paolicchi, A., Scarano, S., Minunni, M. 2022. A biomimetic enzyme-linked immunosorbent assay (BELISA) for the analysis of gonadorelin by using molecularly imprinted polymer-coated microplates. Anal Bioanal Chem. Online ahead of print 13-01-22. https://doi.org/10.1007/s00216-021-03867-7.

Tsoukalas, N., Kiakou, M., Tsapakidis, K., Tolia, M., Aravantinou-Fatorou, E., Baxevanos, P., Kyrgias, G., Theocharis, S., 2019. PD-1 and PD-L1 as immunotherapy targets and biomarkers in non-small cell lung cancer. JBUON 24, 883-888.

Yin, Y., Yan, L., Zhang, Z., Wang, J., 2015. Magnetic molecularly imprinted polydopamine nanolayer on multiwalled carbon nanotubes surface for protein capture. Talanta 144, 671-679.

Zhao, C., Hellman, L. M., Zhan, X., Bowman, W. S., Whiteheart, S. W., & Fried, M. G., 2010. Hexahistidine-tag-specific optical probes for analyses of proteins and their interactions. Anal. Biochem. 399, 237-245.

Zhang, M.M., Huang, R.Y, Beno, B.R, Deyanova, E.G, Li, J., Chen, G., Gross, M.L., 2020. Epitope and Paratope Mapping of PD-1/Nivolumab by Mass Spectrometry-Based Hydrogen-Deuterium Exchange, Cross-linking, and Molecular Docking. Anal. Chem. 7, 9086-9094.

Zhang, Z., Liu, Y., Huang, P., Wu, F.-Y., Ma, L., 2021. Polydopamine molecularly imprinted polymer coated on a biomimetic iron-based metal–organic framework for highly selective fluorescence detection of metronidazole. Talanta 232, 122411.

Zhu, X., Lang, J., 2017. Soluble PD-1 and PD-L1: predictive and prognostic significance in cancer. Oncotarget 8, 97671-97682.

Zhou, J., Mahoney, K.M., Giobbie-Hurder, A., Zhao, F., Lee, S., Liao, X., Rodig, S., Li, J., Wu, X., Butterfield, L.H., Piesche, M., Manos, M.P., Eastman, L.M., Dranoff, G., Freeman, G.J., Hodi, F.S., 2017. Soluble PD-L1 as a Biomarker in Malignant Melanoma Treated with Checkpoint Blockade. Cancer Immunol Res. 5, 480-492.

Supplementary Material

Click here to access/download

Supplementary Material

Supplementary material.docx

Highlights

- A 3K toolbox-based strategy for triggering epitope imprinting technology inside a polynorepinephrine matrix is developed
- ‘AK’ model epitopes are designed by inserting a Lys triplet, gradually mutating its relative position and distance along the sequence
- The binding capacities of the ‘AK’ peptides versus the relative MIP were tested by Surface Plasmon Resonance
- The method has been successfully applied to a real diagnostic case: soluble PD-L1 detection
- Soluble PD-L1 is under consideration as a promising cancer biomarker in liquid biopsies
- A highly sensitive MIP-based sensing assay is established for soluble PD-L1 detection in human serum

Declaration of interests

☒ The authors declare that they have no known competing financial interests or personal relationships that could have appeared to influence the work reported in this paper.

☐The authors declare the following financial interests/personal relationships which may be considered as potential competing interests:

Conflict of Interest and Authorship Conformation Form

Please check the following as appropriate:

⌀ All authors have participated in (a) conception and design, or analysis and interpretation of the data; (b) drafting the article or revising it critically for important intellectual content; and (c) approval of the final version.

⌀ This manuscript has not been submitted to, nor is under review at, another journal or other publishing venue.

⌀ The authors have no affiliation with any organization with a direct or indirect financial interest in the subject matter discussed in the manuscript

○ The following authors have affiliations with organizations with direct or indirect financial interest in the subject matter discussed in the manuscript:

Author's name	Affiliation
Francesca Torrini	University of Florence/ Chemistry Department
Giada Goletta	University of Florence/ Chemistry Department
Pasquale Palladino	University of Florence/ Chemistry Department
Simona Scarano	University of Florence/ Chemistry Department
Maria Minunni	University of Florence/ Chemistry Department